Enabling Transcranial Electrical Stimulation via STI01: Experimental Simulations and Hardware Circuit Implementation

Guanjie Xu[1]
School of Advanced Technology, Xi'an Jiaotong-Liverpool University, Suzhou, Jiangsu, China
Guanjie.Xu22@student.xjtlu.edu.cn

Gaomin Su[1]
Suzhou Linghuier Technology Co., Ltd., Suzhou, Jiangsu, China
sgmcy@126.com

Hao Fang[2]
Suzhou Linghuier Technology Co., Ltd., Suzhou, Jiangsu, China
fanghao0506@qq.com

Yue Li[*]
Department of Computing, School of Advanced Technology, Xi'an Jiaotong-Liverpool University, Suzhou, Jiangsu, China
[*]Corresponding author: yue.li@xjtlu.edu.cn

***Abstract*—This paper presents the novel utilization of a chip, STI01, developed in China and traditionally used for muscle stimulation, to meet the demands of transcranial electrical stimulation (tES). We present the principles behind the design of the external circuit's filter, along with the simulation results. Notably, we successfully accomplished tES utilizing the STI01 chip. This design could be enhanced further by enriching the MCU (STM32F030) program and introducing a closed-loop Brain-Computer Interface (BCI). Given the compact nature of the circuit design, it has potential for integration as a core circuit in portable wearable devices.**

Keywords: STI01; filter design; simulation; tES; closed-loop BCI

I. Introduction

Transcranial electrical stimulation (tES) is an important feedback tool, where micro-currents (0-2mA) are applied to specific areas of the brain in a non-invasive manner, leading to changes in the excitability of nerve cells and the activity of cortical neurons, and thus triggering changes in brain function [1]. tES has been shown to improve the quality of brain-computer interface (BCI) signals and to enhance motor imagery or attention, thereby increasing the accuracy and speed of control commands [2], and can also be used as a means of neuromodulation in BCI [3].

Figure 1 shows the flow of the closed-loop BCI neuromodulation, and their respective names. The computer takes electrical signals from the brain through non-invasive electrodes and converts them into the electroencephalogram (EEG). The computer extracts biological features, uses machine learning for neurological disorder detection, and applies tES for neuromodulation.

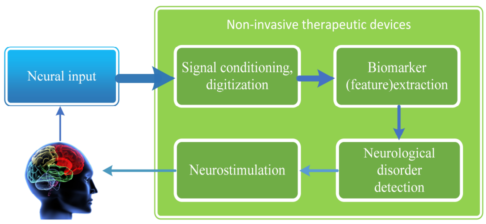

Figure 1. Schematic diagram of a closed-loop BCI system

Based on closed-loop BCI neuromodulation, this paper introduces an external circuit design that allows for tES effects building on the electrical stimulation chip STI01. Experiments and tests were carried out to evaluate the performance.

II. Related Work

tES is a non-invasive brain stimulation method that administers specific low-intensity currents to targeted brain regions via electrodes. It is capable of modulating synaptic plasticity and altering cortical excitability, thereby regulating neuronal activity in the brain. The primary methods of tES include transcranial direct current stimulation (tDCS), transcranial alternating current stimulation (tACS) and transcranial random noise stimulation (tRNS) [4].

Nitsche et al. [5] explored the potential of cathodal direct current stimulation in inducing prolonged excitability reductions in the human motor cortex. They reported that neuron specific enolase concentrations, a marker for neuronal damage, remained stable throughout the experiment, suggesting the safety of the stimulation protocol. Mohebbian et al. [6] found that it improved sleep and increased resilience by applying tES to the brain. Alizadeh Goradel et al. [7] demonstrated that tES was effective in treating depression and anxiety. Bin Altaf et al. [8] developed a chip for tES, which is fully functional and adaptive, but has a complex design and high cost.

Current chips for tES, such as the LM334 chip, have a single mode, tDCS only. The chip designed in this study provides a cost-effective alternative. It is not only safe and reliable, but also meets the requirements of tES at a significantly reduced cost.

III. Hardware Circuit Implementation

Figure 2 shows the electrical stimulation chip STI01, which was developed by Suzhou Linghuier Technology Co., Ltd. The digital circuit is driven by VL and the analogue circuit by VH, allowing the direction of the stimulation current to be switched. AIN, BIN, EN are signal inputs, VL is the low voltage input, VH is the high voltage input, AO, BO are outputs.

2023 5th International Conference on Electronic Engineering and Informatics (EEI) | 979-8-3503-2707-6/23/$31.00 ©2023 IEEE | DOI: 10.1109/EEI59236.2023.10212634

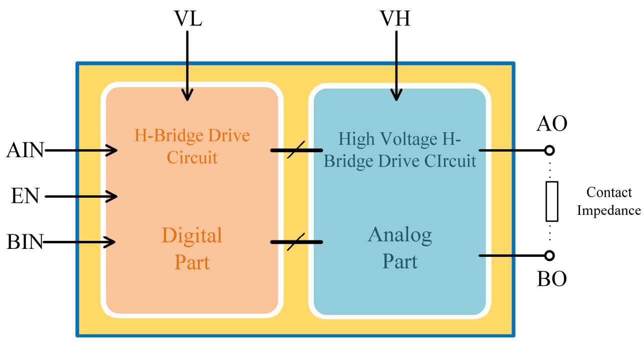

Figure 2. STI01 chip structure diagram

A. Performance

The STI01 chip is mainly used for muscle stimulation and its characteristics include

1) Power supply: VH (max) = 120V; VL (max) = 5V
2) Maximum current: 60mA
3) Overcurrent detection output
4) Switching of stimulation current direction
5) Constant voltage stimulation
6) Digital supply voltage of 3.3-5V, analogue supply voltage of 20-120V
7) Built-in overcurrent detection impedance with a resistance of 10Ω
8) Operating temperature range (0-85°C)

B. Design Scheme

This design includes the construction and debugging of hardware modules and the writing of software programs in addition to the STI01. It further involves circuit simulation, design, and realization predicated on the outcomes of these simulations, and the crafting of an auxiliary circuit utilizing the STI0l chip. The hardware circuit mainly includes the MCU control module, the boost module and the STI01 module. Software program writing including output trigger signal, departure frequency, intervention time setting and interrupt triggering.

1) MCU

The MCU (STM32F030) is used as the main control chip with a 32-bit RISC core, up to 48MHz operating frequency, high-speed embedded memory, and a wide range of enhanced peripherals and I/O ports, seven general-purpose 16-bit timers and an advanced control PWM timer. The trigger signal is output via the MCU.

2) STI01 Chip

The VL port is powered by a 3.3V power supply, which is boosted by a boost module to power the VH port. The MCU PA10, PB1 is connected to the STI01 chip AIN, and BIN port, PF1-OSC-OUT is connected to the EN port, and PA5 is connected to the I/O port.

IV. Experimental Simulations

A. Software functions

The MCU as the core control circuit has to control each circuit module, including the initialization of the chip in the circuit and the overvoltage detection. When the voltage detected by the I/O port exceeds the set threshold voltage, an interrupt is output. As shown in Figure 3.

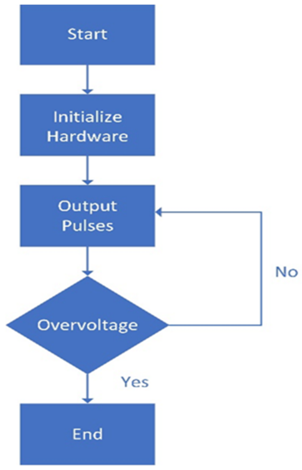

Figure 3. Software design flowchart

B. Output test results

The 3.3V supply voltage supplies the MCU and low voltage side of STI01, the high voltage side of STI01 is supplied at 20V and the impedance load is 10KΩ. The test results are as follows:

1) When a pulse wave of 3.3V pulse width 200us is input to the STI01's AIN, the AO outputs a pulse wave of approximately 23V pulse width 200us.

2) When a pulse wave with an amplitude of 3.3V and a pulse width of 200us is input to the BIN of the STI01, the BO outputs a pulse wave of approximately 18V.

As shown in Figure 4, the top left shows the AO output, which is a pulse waveform. The top right is a zoomed-in view of the pulse waveform, which is visible as not a flat-topped pulse wave. Bottom left is the BO output, which is similar to the AO output. Bottom right is a larger image of the BO pulse waveform.

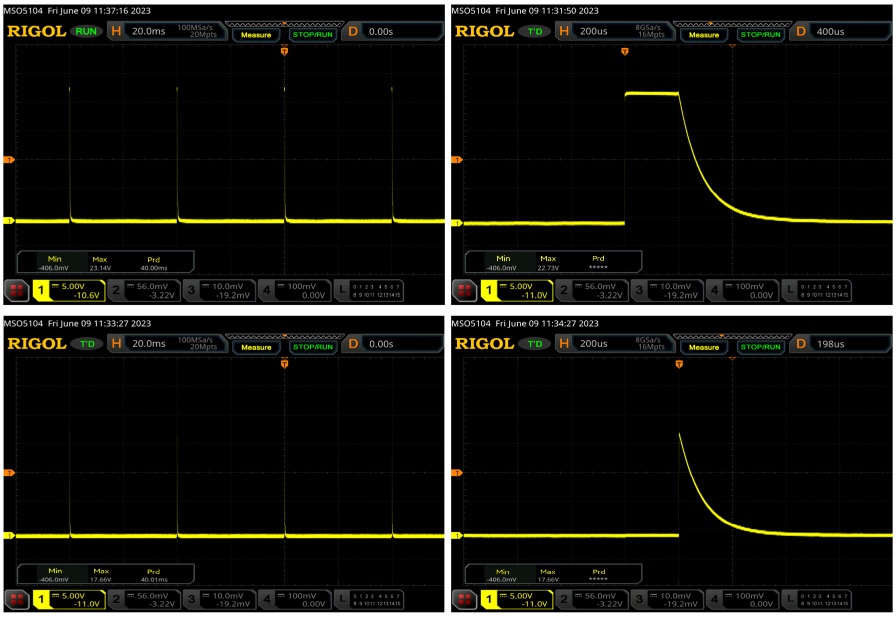

Figure 4. Output voltage

C. Simulation circuit construction

In order to simulate the pulse generated by STI01, an analog circuit with a similar output was built, and the output of this circuit was designed through a circuit to achieve rectification of the pulsed current waveform into a current that satisfies tDCS, as shown in Figure 5.

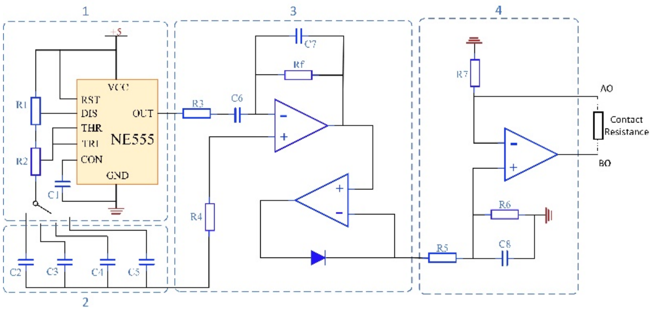

Figure 5. Schematic diagram of the analogue circuit

The first segment, through the timer IC output rectangular PWM wave, by adjusting the second segment of the capacitor combination, change the output frequency, through the third segment, rectify the rectangular wave transmission into a pulse wave, its output is similar to STI01 chip, the formulas are as follows:

$$U_{in} = \left(\frac{A}{2}\right) * sign\left\{\sin\left(\frac{2\pi t}{T}\right)\right\} + \left(\frac{A}{2}\right) \quad (1)$$

$$U_{out} = -RC\frac{dU_{in}}{dt} \quad (2)$$

Equation (1) is the input rectangular pulse expression, A is the pulse amplitude and T is the pulse period, t is the time. Equation (2) is the differentiation of the input quantity.

In the fourth segment, the pulse current is transformed into a steady output current, with a magnitude ranging from 0 to 2mA. A representation of this simulated output is depicted in Figure 6. Where the top diagram shows the pulse current and the output is similar to the STI01. The lower diagram shows the output current after the filtering circuit, which satisfies the 0 to 2mA DC needed for tDCS.

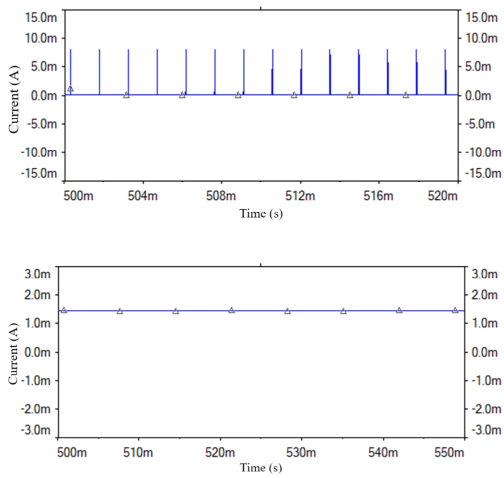

Figure 6. Simulation output showing the STI01 pulse current (top) being converted to a steady current that is ready to use for tDCS (bottom)

Table I illustrates the outcomes of rectified output following the passage through a filter circuit under varying pulse frequencies. The decrease in pulse current as the pulse frequency increases, from 40.592mA at 100Hz to 5.975mA at 1000Hz, suggests the effectiveness of the filter in pulse current regulation. Despite these changes in pulse current, the output current remains relatively stable, indicating the filter's ability to maintain a consistent output in the face of varying frequencies.

TABLE I. SIMULATED OUTPUT CURRENT AT A LOAD IMPEDANCE OF 10KΩ

Pulse frequency	**Pulse current**	**Output current**
100Hz	40.592mA	1.505mA
400Hz	12.293mA	1.506mA
700Hz	7.656mA	1.514mA
1000Hz	5.975mA	1.554mA

Table II, on the other hand, presents the rectified results post-filtering under different load impedances, with a constant frequency of 10Hz. The minor fluctuations in pulse current across the range of load impedances, coupled with the exceptional stability of the output current, underscore the filter's ability to deliver a consistent output under different load conditions.

TABLE II. SIMULATED OUTPUT CURRENTS AT A FREQUENCY OF 10 HZ

Load impedance	**Pulse current**	**Output current**
1KΩ	7.308mA	1.291mA
5KΩ	7.713mA	1.291mA
10KΩ	7.494mA	1.283mA
15KΩ	6.827mA	1.289mA
20KΩ	6.805mA	1.291mA

Following the comprehensive analysis results shown in Tables I and Tables II, it can be concluded that the filter circuit design is successful, satisfying the output of 0 to 2mA DC current at different frequencies and different impedances. Therefore, it can be applied to the STI01.

D. Circuit design ideas based on the STI01 chip

Based on output test analysis, the STI01 chip output is a periodic pulse wave, while the tDCS needs to meet the 0-2mA DC current output. Therefore, the design of the original circuit needs to meet the following requirements:

1) Processing of pulse currents such as rectification and filtering.

2) Satisfaction of tDCS requirements.

3.3V DC voltage is used to power the MCU and the VCC port of the STI01 chip, and a boost circuit is used to increase the voltage to 20V to power the VDD port of the STI01 chip. The MCU PA10 and PB1 provide the trigger voltage for the STI01 chip. An RC filter circuit is connected between the output ports AO and BO and R2 can be considered as the contact impedance.

For specific connections, please refer to Figure 7.

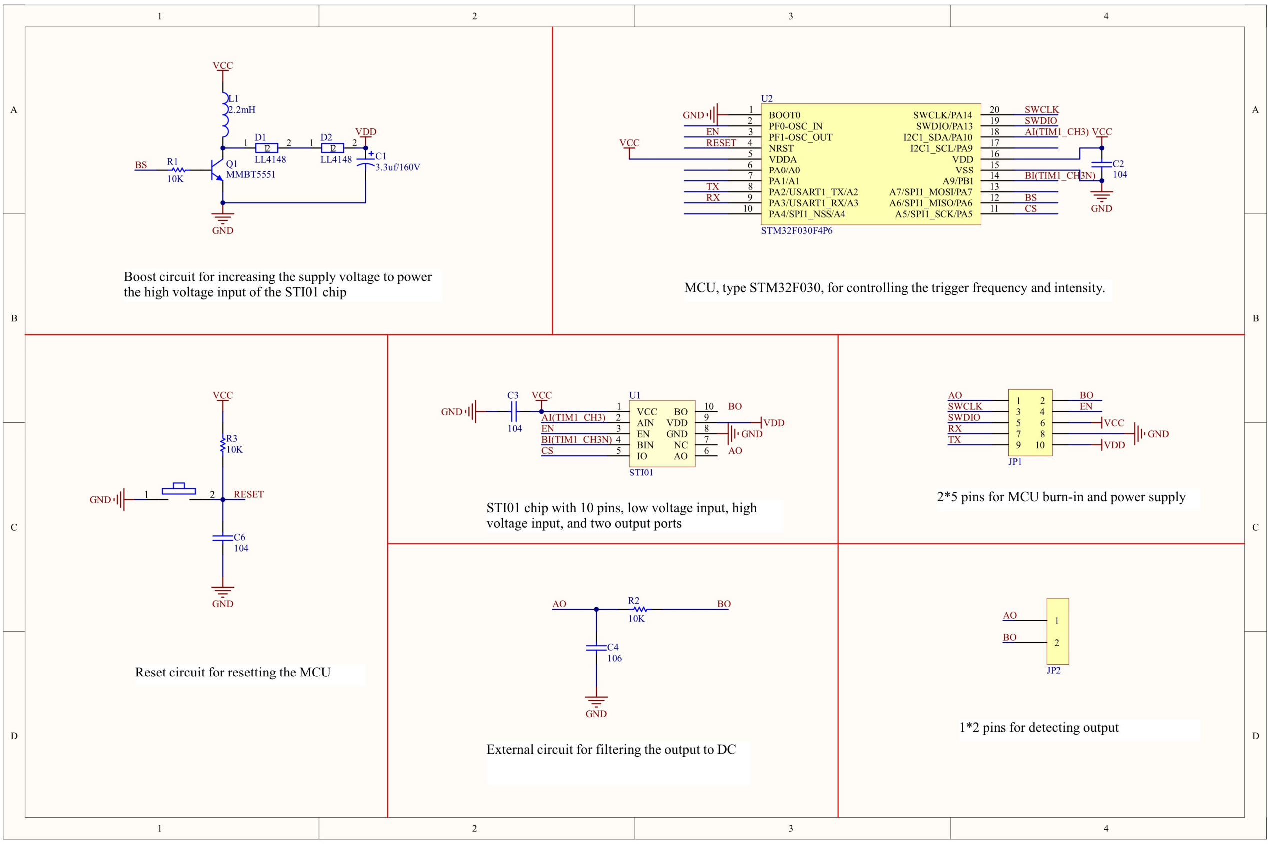

Figure 7. Based on STI01 overall circuit design

E. STI01 chip enables tDCS testing

The MCU and the low-voltage side of the STI01 are supplied with a voltage of 3.3V. The high-voltage side of the STI01 is supplied with a voltage of 20V. With a load of 10KΩ, the output structure is illustrated in Figure 8.

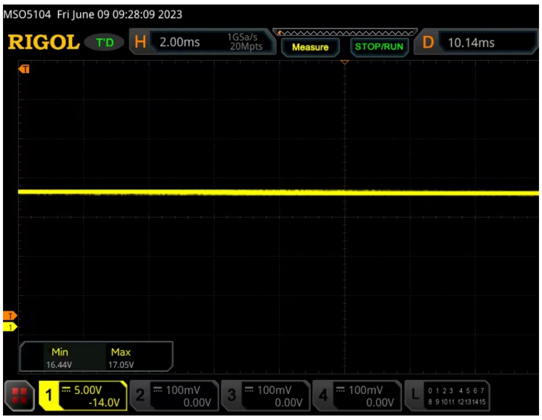

Figure 8. Output after external circuitry

Since the load impedance is 10kΩ and the voltage is 17.05V, so the current is 1.705mA and the error is

$$\varepsilon = \frac{I - I_{real}}{I_{real}} \times 100\%$$

In the formula I is the deviation amount, I_{real} is the base amount, we can get the error of 3.7%.

F. Possibility of implementing tRNS based on SIT01

As with tDCS, the tRNS is a non-invasive brain stimulation technique that is a form of tES. tRNS was first investigated in humans by Terney et al. [9]. It was demonstrated that tRNS increases motor cortex excitability (i.e. increases the amplitude of motor evoked potentials). In addition, several scientists have found that high frequency tRNS (101Hz to 640Hz) is beneficial in reducing pain in multiple sclerosis, in reducing motor cortical excitability in Parkinson's disease, and in reducing depressive symptoms and improving negative symptoms in schizophrenia [10].

By testing the current from the AO to the BO it can be found that the current is a high frequency random noise current, as shown in the Figure 9.

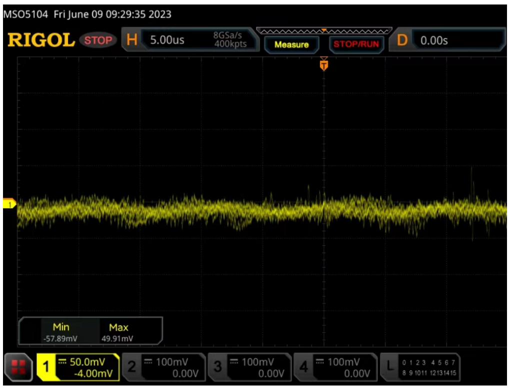

Figure 9. AO to BO output

However, the output current is low, probably because the voltage value supplied to the high-voltage H-bridge drive circuit is not high enough. This issue requires further research and discussion.

V. Conclusion and Future Work

In this study, we exploit the capabilities of an existing tES chip, the STI01, known for its low-cost, safe and reliable output stability with overvoltage detection for muscle stimulation. Utilizing an external circuit design with the STI01 chip, we successfully implement tES. Through simulation, its feasibility is verified and through testing it is found that after the circuit design not only tDCS can be achieved, but also the possibility of achieving tRNS exists. However, subsequent work will need to adjust the program of the MCU to perfect or increase the voltage, so that the tRNS output can reach an adjustable functionality, ultimately enriching the control over the STI01 chip.

Additionally, the compact and convenient design of this circuit makes it a suitable candidate for embedding into wearable devices. Future refinements are envisioned in areas such as the human-machine interface, output adjustments, and achieving better system integration, as well as in stimulus focusability, stimulus depth, and positioning control for the tES system.

References

[1] B. Z. Allison, E. W. Wolpaw, and J. R. Wolpaw, 'Brain–computer interface systems: progress and prospects', Expert Review of Medical Devices, vol. 4, no. 4, pp. 463–474, Jul. 2007.

[2] E. Santarnecchi, A.-K. Brem, E. Levenbaum, T. Thompson, R. C. Kadosh, and A. Pascual-Leone, 'Enhancing cognition using transcranial electrical stimulation', Current Opinion in Behavioral Sciences, vol. 4, pp. 171–178, Aug. 2015.

[3] Ren Xu et al., 'A Closed-Loop Brain–Computer Interface Triggering an Active Ankle–Foot Orthosis for Inducing Cortical Neural Plasticity', IEEE Trans. Biomed. Eng., vol. 61, no. 7, pp. 2092–2101, Jul. 2014.

[4] W. Paulus, 'Transcranial electrical stimulation (tES – tDCS; tRNS, tACS) methods', Neuropsychological Rehabilitation, vol. 21, no. 5, pp. 602–617, Oct. 2011.

[5] M. A. Nitsche, M. S. Nitsche, C. C. Klein, F. Tergau, J. C. Rothwell, and W. Paulus, 'Level of action of cathodal DC polarisation induced inhibition of the human motor cortex', Clinical Neurophysiology, vol. 114, no. 4, pp. 600–604, Apr. 2003.

[6] B. Mohebbian, M. Najafi, and P. Sabahi, 'The effect of transcranial direct current stimulation on sleep quality, resilience, and optimism', Curr Psychol, vol. 42, no. 7, pp. 5785–5792, Mar. 2023.

[7] J. Alizadeh Goradel, A. Pouresmali, M. Mowlaie, and F. Sadeghi Movahed, 'The Effects of Transcranial Direct Current Stimulation on Obsession-compulsion, Anxiety, and Depression of a Patient Suffering from Obsessive-compulsive Disorder', PCP, vol. 4, no. 2, 2016.

[8] M. A. Bin Altaf, C. Zhang, and J. Yoo, 'A 16-Channel Patient-Specific Seizure Onset and Termination Detection SoC With Impedance-Adaptive Transcranial Electrical Stimulator', IEEE J. Solid-State Circuits, vol. 50, no. 11, pp. 2728–2740, Nov. 2015.

[9] D. Terney, L. Chaieb, V. Moliadze, A. Antal, and W. Paulus, 'Increasing Human Brain Excitability by Transcranial High-Frequency Random Noise Stimulation' J. Neurosci., vol. 28, no. 52, pp. 14147–14155, Dec. 2008.

[10] O. Van Der Groen and N. Wenderoth, 'ranscranial Random Noise Stimulation of Visual Cortex: Stochastic Resonance Enhances Central Mechanisms of Perception' J. Neurosci., vol. 36, no. 19, pp. 5289–5298, May,2016.